



Intense Pulsed Light unprinting for reducing life-cycle stages in recycling of coated printing paper

Michael Dexter ^a, Keri Rickman ^a, Changqing Pan ^b, Chih-hung Chang ^b, Rajiv Malhotra ^{a,*}

^a Department of Mechanical and Aerospace Engineering, Rutgers University, 98 Brett Road, Piscataway, NJ 08854, USA

^b School of Chemical, Biological and Environmental Engineering, Oregon State University, 105 SW 26th St #116, Corvallis, OR, 97331, USA

ARTICLE INFO

Article history:

Received 9 December 2018

Received in revised form

1 May 2019

Accepted 30 May 2019

Available online 31 May 2019

Keywords:

Paper

Recycling

Unprinting

Intense Pulsed Light

ABSTRACT

Unprinting of paper can reduce multiple life-cycle stages in the recycling of paper to yield significant environmental impact. Laser-unprinting has been demonstrated for uncoated paper but causes significant damage to coated paper. This work explores a scalable optical (non-laser) process for unprinting coated paper. Printed coated paper is exposed to pulsed broad-spectrum Intense Pulsed Light (IPL) from a xenon lamp and the toner is then removed by dabbing gently with an ethanol wipe. While black toner is easily unprinted, unprinting of colored prints (red, blue, green) is best realized by incorporating an initial overprint of black toner. An unprinting throughput on the order of mm^2/s is achieved. Three distinct regimes of unprinting are identified based on the extent of toner removal and damage of the paper. The optical properties of the unprinted paper, characterized via UV–Visible spectrophotometry, are correlated to these regimes to understand the potential for in-situ optical process monitoring. Scanning Electron Micrography and Fourier-Transform Infrared Spectroscopy are performed to understand the underlying mechanisms that govern the occurrence of the different unprinting regimes. Further, the potential impact of the developed approach on recycling of paper is discussed in the context of the capabilities of current optical unprinting approaches and the potential elimination of life-cycle stages in conventional paper recycling.

© 2019 Elsevier Ltd. All rights reserved.

1. Introduction

Production of pulp, paper, paperboard and wood products is a major contributor to climate change emissions, chemical pollution, and energy usage (Tong et al., 2018), e.g., total carbon emissions from this industry have been estimated as equivalent to 12 GtCO₂ (Metz et al., 2007) and paper and pulp production forms the lion's share ($\approx 42\%$) of global industrial wastewater production. Conventional paper recycling is aimed primarily at reducing the impact of paper usage on woodlands and involves the breakdown and reconstitution of the paper, via the following steps.

First, the recyclable paper is moved from the point-of-use to the point-of-recycling where it is classified according to paper type and ink type. This step involves the energy used in transporting the paper but is a relatively smaller contributor to energy usage, climate change emissions and pollution. The paper is converted back to a pulp stage (i.e., pulping stage) using mechanical, chemical

or thermomechanical methods to form a slurry and to detach the toner particles from the fibers. This step is one of the largest consumers of energy and releasers of climate change gases within the recycling step (Ahmadi et al., 2003; Counsell and Allwood, 2007; EIPPCB, 2001). The detached ink is removed from the pulp by washing or flotation or screening or centrifugal separation (i.e., deinking step) followed by bleaching to improve visual appearance (Tsatsis et al., 2017). This step is typically one of the largest contributors to chemical pollution of waste water streams (Bajpai, 2014; Jiang and Ma, 2000). The paper pulp is dried and reconstituted into printable paper sheets, along with any coatings needed. This stage of recycling is the second largest contributor to energy usage after the pulping step and the largest contributor to climate change emissions relative to the above steps (Ahmadi et al., 2003; Counsell and Allwood, 2007; EIPPCB, 2001).

Thus, the conventional recycling approach is still a major contributor to energy usage, climate change emissions and toxic chemicals released into the environment (Energetics Incorporated Columbia, 2005). Approaches for increasing the efficiency and reducing the environmental impact of the above life-cycle include modification of the deinking pulping process (Man et al., 2017;

* Corresponding author.

E-mail address: rajiv.malhotra@rutgers.edu (R. Malhotra).

Nathan et al., 2018) and improved valorization of the by-products from paper production (Singh et al., 2018; Tesfaye et al., 2017). However, this approach does not lead to removal of any life-cycle steps and its impact is therefore relatively small. Another approach is the replacement of paper with an electronic equivalent, which can completely eliminate all of the above life-cycle steps. It has been estimated that electronic paper can reduce climate change emissions by nearly 85% and reduce energy consumption by nearly 52% (Counsell and Allwood, 2007). Even greater reductions can be enabled by the unprinting of paper, i.e., 95% and 86% respectively (Counsell and Allwood, 2007) again via elimination of all the above life-cycle stages in conventional recycling. Unprinting is a paper recycling approach in which the ink is directly removed from the printed paper without damaging the paper in any way. Unprinting is conceptually distinct from deinking because it does not need prior pulping of the paper, can be performed with simple tools that are easy to integrate with paper printers, and uses minimal amount of chemicals. When realized in this form unprinting can reduce or eliminate all the above described life-cycle stages in conventional paper recycling and realize a new level of point-of-use recycling and reuse.

Given the above potential, various approaches have been explored for effecting unprinting (Counsell and Allwood, 2006) and are summarized here. Adhesion-based unprinting (Yoshie and Taniguchi, 2000) presses a material, that forms a stronger bond with the toner than that between the toner and the paper, against the printed paper and then peels it off to remove the toner. This method often requires significant chemical pre-processing to weaken the toner-paper bond followed by physical means of toner removal, both of which can damage the paper. The abrasion-based method (Hirai, 2002) uses abrasive particles to apply oscillating mechanical energy to remove the toner, but the potential for mechanically damaging the paper itself is high. Solvent-based unprinting (Bhatia et al., 1999; Boyce et al., 2001) exposes the printed paper to organic chemicals that selectively dissolve the toner but not the paper. The need for significant amount of these chemicals, which are often environmentally harmful, places an additional environmental burden. In the decoloring approach, printing is performed using specialized inks that change color and become transparent to the eye upon exposure to heat or UV radiation (Mitsubishi et al., 1994). This process requires specialized and expensive paper and places restrictions on the printing process and toner used.

Unprinting via toner ablation using a laser has been demonstrated, with significant advances in understanding and feasibility achieved recently (Counsell and Allwood, 2008; Leal-Ayala et al., 2011, 2012). The key advantages of this approach include low chemical usage, no need for specialized inks or paper, and elimination of mechanically-induced damage of the paper. The ease of integration of lasers with existing printers also makes it amenable to realizing the full advantages of unprinting. Optimum laser parameters were derived to successfully remove toner from uncoated paper printed using various laser printers with characterization of unprinting being performed using analysis of micromorphology, chemical composition and optical appearance. However, laser light invariably damaged the coating layer during unprinting of coated paper, thus impairing its reuse. In a typical coated printing paper the base cellulose fibers are sandwiched by a protective layer consisting of a combination of polymer resins and other silica-based minerals (e.g. Kaolin). This provides the paper with a glossy appearance, makes it smoother, and provides greater opacity for enhanced printing quality in advertising, packaging, books, photographs, cups and holders, and offset printing applications (Lehtinen, 2000). Given that coated paper comprises nearly 40% of the current global production of printing paper (Nations, 2016),

optical unprinting of such paper with minimal chemical usage and high scalability can have a significant impact on sustainability in paper recycling.

This work explores a new process for optical unprinting of coated paper without using a laser. This process uses large-area, pulsed and broad-spectrum visible light from a xenon lamp (i.e., Intense Pulsed Light or IPL) incident on the paper, followed by usage of very low quantity of environmentally benign ethanol (i.e., an ethanol wipe) to remove the toner. Distinct unprinting regimes are identified by analyzing the paper's appearance and optical reflectance. The microstructure and surface chemistry of the unprinted paper are examined to uncover the mechanisms underlying these regimes. The potential of this process for high throughput unprinting and its role in reducing the environmental impact of paper recycling is discussed. We note that IPL has been used in the past for fusing conductive nanomaterials on substrates like paper, polymers and fabrics for applications in flexible and rigid electronics (Bansal and Malhotra, 2016; Dexter et al., 2018; Dharmadasa et al., 2013; Greenberg et al., 2017; Jha et al., 2015; Kang et al., 2014; MacNeill et al., 2015; Wan-Ho et al., 2013). While this use of IPL is known to be scalable due to its large area capability and minimal damage to the underlying substrates, there has been no investigation till date on using IPL for unprinting.

2. Materials and methods

Semi-gloss coated paper (grade 0.27 mm thick, weight 270 g/m²) was printed using a Xerox 7845 multicolor printer. The test samples consisted of bars of black, blue, red and green colors (Fig. 1a) printed with Xerox toner numbers 00612015-09 to 00612015-12. The samples were exposed to pulsed light from a xenon flash lamp (Sinteron 3000, Xenon Corp.), as shown in Fig. 1b. The samples were placed 1.5 inches from the lamp surface so that the optical footprint on the plane of the sample was approximately 12 inch × 1.5 inch. The power spectrum of this lamp ranges from 350 nm to 800 nm, with most of the energy concentrated in the 400–700 nm region (Fig. 1c). This power spectrum avoids light in the UV and IR regions, which damages the paper as observed in past work on laser unprinting (Leal-Ayala et al., 2011). The total incident fluence F was calculated using Equation (1), as specified by the lamp manufacturer. In this equation V is the voltage (in kV) supplied to the capacitors that charge the xenon lamp and t is the pulse on time (in microseconds). In our experiments V was fixed at 3 kV and t was varied to get a range of optical fluences. Note that this approach effectively amounts to changing the irradiation time for the same irradiance, with greater fluence obtained by increasing the irradiation time. Here, we report results in terms of the fluence and pulse number since this is the usual combination of process parameters used in conventional IPL sintering (Bansal and Malhotra, 2016; Dexter et al., 2018; Jha et al., 2015; Wan-Ho et al., 2013). After exposure to IPL the surface of the paper was lightly dabbed with an ethanol wipe to remove the toner, thus changing the visual appearance by exposing the underlying paper coating. The paper color did not change without using the ethanol wipe after pulsed light exposure. Using the wipe before pulsed light exposure had no effect either.

The surface morphology of the samples was examined using a Scanning Electron Microscope (SEM, Zeiss Sigma Field Emission 8100). The optical reflectance of the samples in the 400–700 nm wavelengths was examined using a Jasco UV–Vis Spectrophotometer with a 60 mm integrating sphere. The angle of incidence during measurement was approximately 5° and the reference material was spectralon (99% reflectance). The measured reflectance spectra indicates the light intensity at various wavelengths received by the human eye when viewing the paper, and is used here as an optical

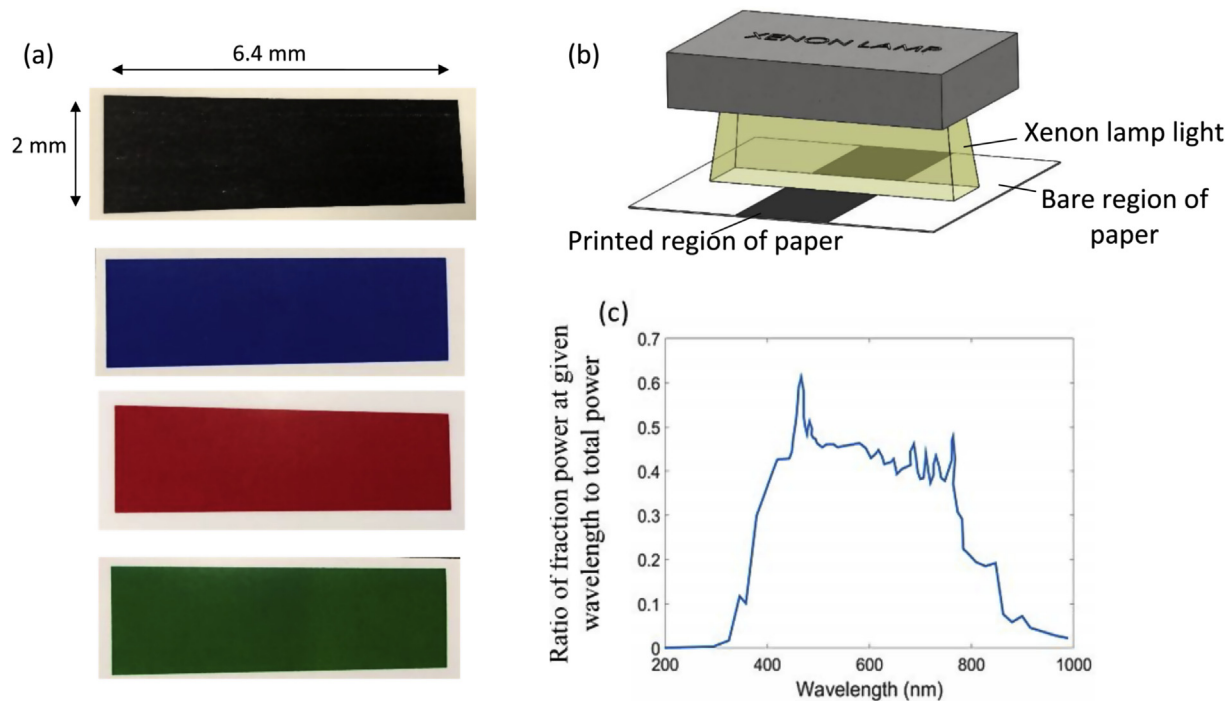


Fig. 1. (a) Images of printed samples (b) Schematic of IPL unprinting (c) Power spectrum of IPL used here.

$$F = \left(\frac{t}{1.5^2} \right) \left(\frac{V}{3120} \right)^{2.4} \quad (1)$$

measure of the degree of unprinting. For example, as discussed in the results section, the bare paper shows very high and uniform reflectance across the visible spectrum whereas the black printed paper shows significantly lower reflectance across the spectrum. The closer the spectrum of the unprinted paper is to that of the bare paper the greater is the degree of unprinting. The deviation in reflectance of the unprinted paper from that of the bare paper was also quantified at the photopic wavelength of 550 nm (Nair and Nair, 1989). The human perception of reflectance is often measured at this wavelength because it corresponds to the maximum luminous intensity received by the cones of the human eye. In addition, Attenuated-Total-Reflectance Fourier-Transform-Infrared-Spectroscopy (ATR-FTIR) of the samples was performed for two purposes. First, to understand the degree of removal of the toner after unprinting, and second to understand the potential mechanism of unprinting by examining the alteration in chemical bonds on the coating. Finally, the unprinted sheets obtained using the optimal processing approach were reprinted using the same toner color and printer, and the change in photopic reflectance examined. This was used to quantify how many times the paper can be reprinted using our approach before reprinting is rendered impossible by paper damage.

3. Results and discussion

We first discuss the visual appearance and optical reflectance of the unprinted paper, followed by SEM and ATR-FTIR results.

3.1. Optical properties

3.1.1. Black prints

Fig. 2a shows examples of the printed and unprinted paper to illustrate various regimes of toner removal. At 7.5 J/cm² fluence a

single pulse does not cause enough toner removal, i.e., the partial-removal regime exists. Increasing the fluence to 10 J/cm² shows a gradual improvement in toner removal with the underlying paper being partially exposed, but still staying within the partial-removal regime. The application of 12 and 13.5 J/cm² pulses achieves good toner removal, i.e., complete-removal. In these cases the color of the unprinted paper is not significantly different from that of the bare paper, a consistent observation wherever complete-removal was achieved in this work. Increasing the fluence to 14.5 J/cm² or greater removes the toner but also causes cracking of the paper, i.e., removal-and-cracking regime. The cracking is confined to the region of the paper where the toner was removed, a consistent observation wherever this regime was observed in this work. These cracks are obviously undesirable and are a process-induced defect that should be avoided.

Fig. 2b shows the corresponding visible reflectance spectra. As expected, the reflectance of the bare paper is very high and is quite uniform across the visible region, whereas the black-printed paper has uniformly low reflectance across the visible spectrum due to significantly higher optical absorption by the toner. In the partial-removal regime (9 J/cm²) the reflectance increases relative to the printed paper, but is nearly 40% lower than that of bare paper at 550 nm. This reflects the visual observation (Fig. 2a) that toner removal is occurring but not to a sufficient degree. When complete removal is achieved (12.5 and 13.5 J/cm²) the reflectance increases significantly, to within 5–6% of the bare paper at 550 nm. Increasing the fluence into the removal-and-cracking regime (14.5 J/cm²) causes a small increase in reflectance, especially below 500 nm. This is despite the appearance of some cracks in the unprinted paper (Fig. 2a). As the fluence increases deeper into this regime (e.g., 18 J/cm²), resulting in the emergence of greater number of cracks, the photopic reflectance reduces to 11% lower than that of the bare paper. These observations indicate that

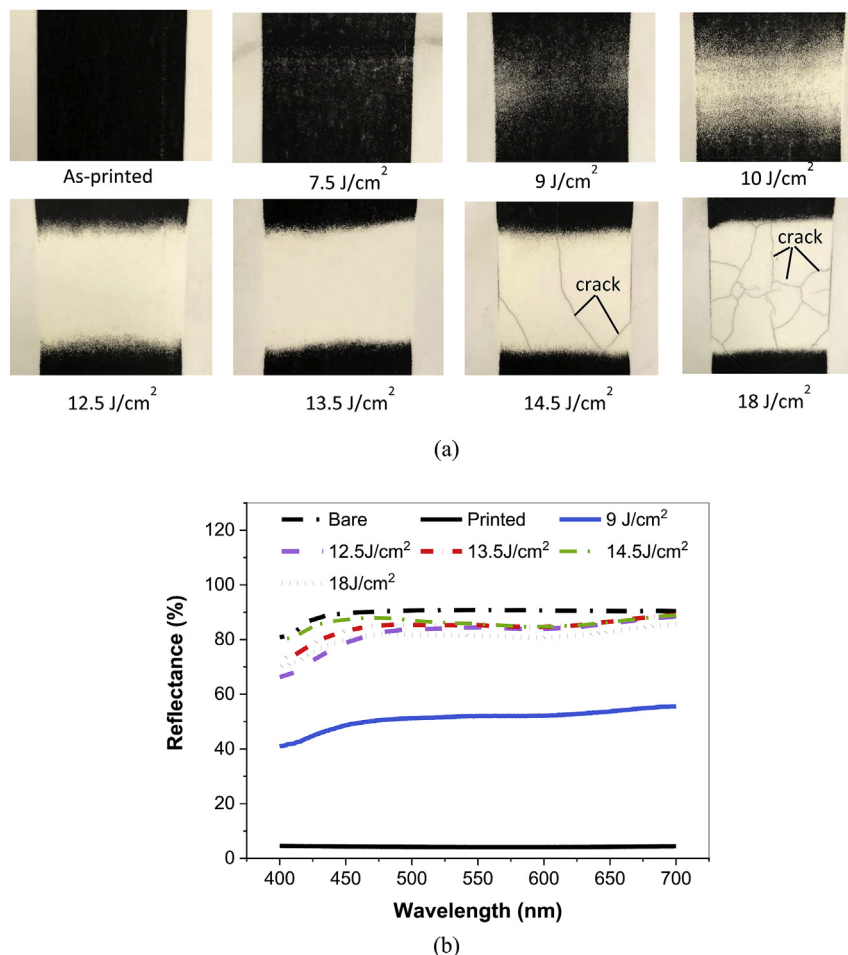


Fig. 2. (a) Representative images of black printed samples in the partial-removal, complete-removal, removal-and-cracking regimes (b) Corresponding reflectance spectra.

increased reflectance can be used as a measure of greater toner removal and subsequently reduced reflection can indicate occurrence of cracking, implying the potential usage of reflectance as an in-line process monitoring tool. However, the caveat is that initiation of cracking will show a significant reduction in reflectance only above a certain amount of crack accumulation. For the above identified single-pulse fluences in the complete-removal regime, multiple pulses were overlapped by in-plane overlap amount *OL* (Fig. 3a), for removal of the entire printed bar. The ethanol wipe was used only after the entire unprinting

process was completed. An example of a successfully unprinted sample is shown in Fig. 3b, for *OL* = 10 mm and fluence 12.5 J/cm². We also observe that using a lower in-plane overlap of 5 mm causes cracking of the paper (Fig. 3c), due to excessive energy incident on the paper in the region between consecutive optical footprints. However, a higher *OL* of 15 mm causes only partial-removal because portions of the paper did not receive enough energy for uniform removal (Fig. 3d).

OL = 5 mm (d) optical image for *OL* = 15 mm. All shown for fluence 12.5 J/cm².

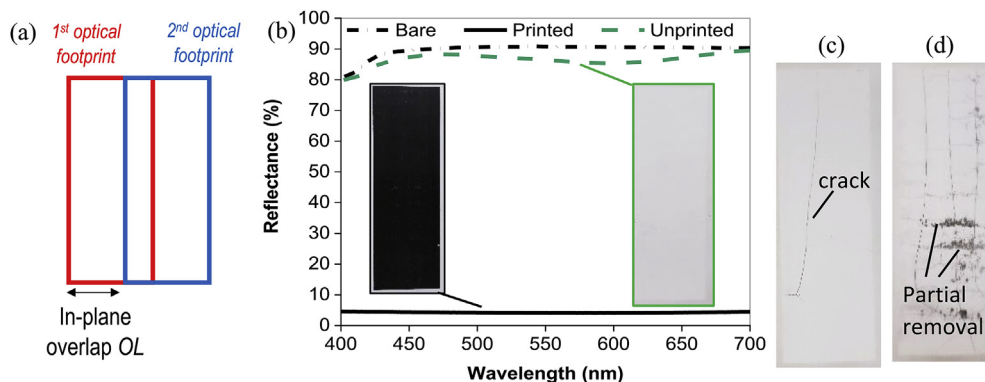


Fig. 3. (a) Schematic of in-plane overlap for unprinting (b) UV-Vis spectra and optical images of printed and unprinted samples with *OL* = 10 mm (c) optical image for

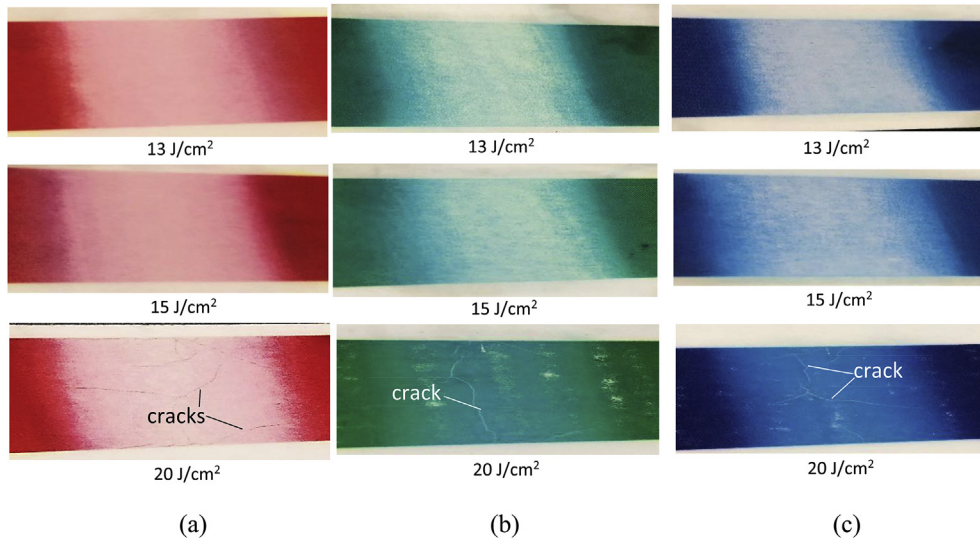


Fig. 4. Optical images of unprinted (a) red (b) green (c) blue samples. (For interpretation of the references to color in this figure legend, the reader is referred to the Web version of this article.)

3.1.2. Colored prints

Fig. 4 shows optical images for printed and unprinted red, green and blue samples. Despite the application of the highest fluence possible with our system only the partial-removal regime or crack occurrence was possible. The lowest deviation in photopic reflectance of these unprinted samples from that of the bare paper was 31%, 24% and 27% respectively. Given that these colored toners have high reflectance peaks at red, green and blue wavelengths (according to the printed color) their absorption of the xenon lamp light is lower than that of the black toner. This is the underlying

reason for an inability to effect enough unprinting. Since we could not find any optical fluence where all the toner could be removed, with or without cracking, this approach is impractical for unprinting. Nonetheless, in contrast to the black prints the colored prints showed a trend in which the occurrence of cracking at higher fluence was accompanied by lesser toner removal, an interesting phenomenon worth examining in future work.

To overcome this issue, we modified the process by printing over the colored prints with black toner and then performing IPL exposure. The goal was to increase absorption by the printed toner

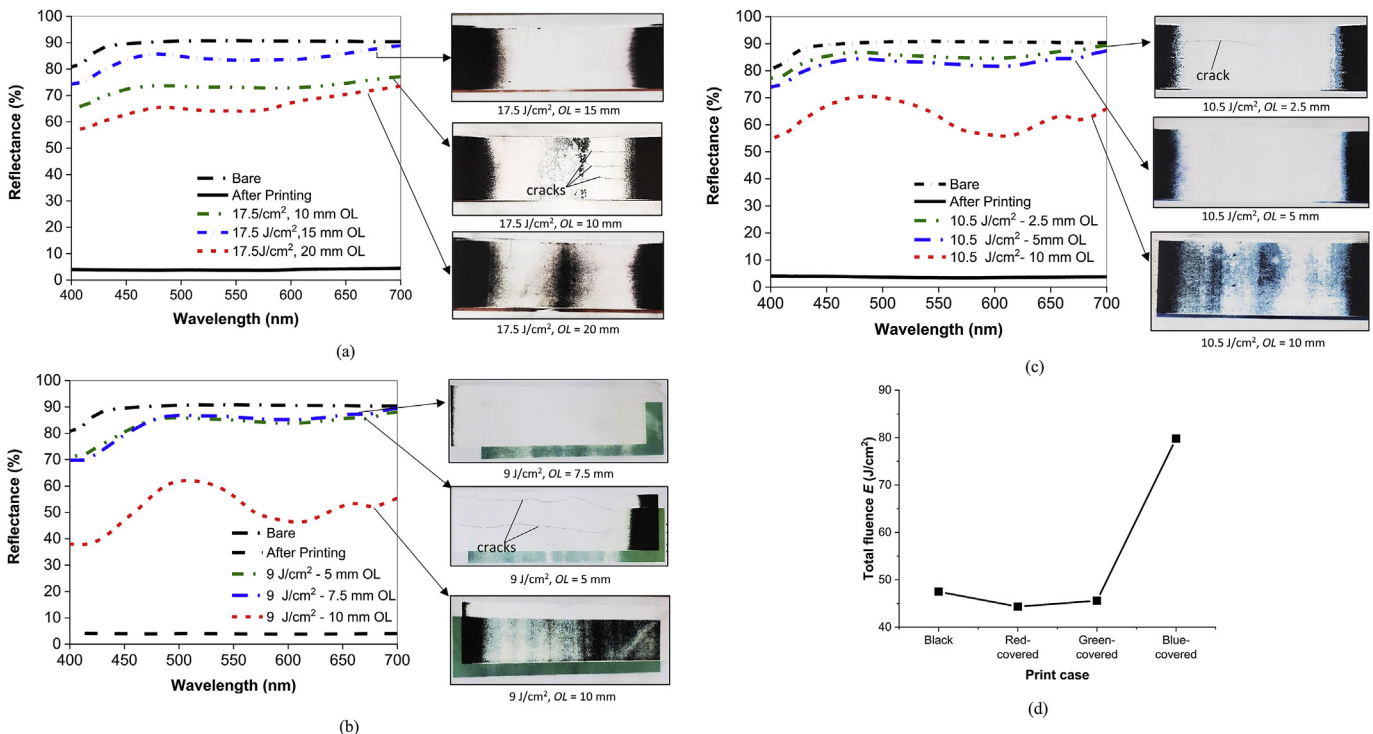


Fig. 5. Reflectance spectra and optical images of samples for (a) red-covered (b) green-covered (c) blue-covered cases. (d) Total fluence E for complete-removal regime, for the different cases examined here. (For interpretation of the references to color in this figure legend, the reader is referred to the Web version of this article.)

Table 1

Combinations of base toner colors used for printed colors.

Printed Color	Toner color combinations
Black	Cyan + Yellow + Magenta + Black
Red	Yellow + Magenta
Green	Cyan + Yellow
Blue	Cyan + Magenta

layers, to an extent sufficient for removal of both the overprinted black toner and the underlying color toner. From this point onwards, we denote such samples as red-covered, blue-covered and green-covered for red, green and blue colors respectively. For these samples we first identified pulse fluences that allowed complete-removal in one optical pulse, and then varied the in-plane overlap. This is because in-plane overlap has a significant impact on the quality of unprinting, as shown for black toner in Fig. 3b–d, even if a single optical pulse without overlapping shows complete toner removal. Further, the penultimate goal of large-area unprinting cannot be realized without using multiple overlapped optical pulses. We note that given the current ability to digitally print paper it would not be a difficult task to print black toner over existing colored patterns on paper before performing unprinting.

Fig. 5 shows the optical images and corresponding reflectance spectra of the unprinted samples. In the red-covered samples (Fig. 5a) a fluence of 17.5 J/cm² with *OL* = 15 mm yielded complete-removal. Reducing the *OL* to 10 mm yielded removal-and-cracking, due to excessive energy deposited in the region common to consecutive pulses. Increasing *OL* to 20 mm resulted in only partial removal of the toner, with the region of unremoved toner between unprinted regions indicating that this portion of the paper did not receive enough energy for unprinting. In the green-covered and blue-covered cases the fluence and in-plane overlap for the complete-removal regime were 9 J/cm²-7.5 mm and 10.5 J/cm²-5 mm respectively, as shown in Fig. 5b and c respectively. Again, an increase in *OL* caused partial-removal and a reduction in *OL* caused removal-and-cracking. The deviation in photopic reflectance of the complete-removal paper from that of the bare paper was 7%, 4% and 5% for the red-covered, green-covered and blue-covered samples respectively. Since this deviation is an order of magnitude lower than that for the colored prints without overprinted black toner, this overprinting strategy is a significantly more effective means of unprinting colored prints.

Fig. 5b–c also show that the dependence of reflectance on the

unprinting regime is similar to that observed for the black prints. In the partial-removal regime the reflectance increases but is not significantly close to that of bare paper. In the complete-removal regime, i.e., at an optimal in-plane overlap, the reflectance increases much more significantly. For the red-covered (Fig. 5a) and green-covered (Fig. 5b) paper in the removal-and-cracking regime the reflectance is reduced as compared to the complete-removal regime. However, for the blue-covered paper (Fig. 5c) the reflectance in the removal-and-cracking regime increases slightly as compared to the complete-removal regime. This observation can be explained by noting that in this regime the number and length of cracks in red-covered and green-covered paper is greater than that in the blue-covered paper. As in the case of the black prints, a significant reduction in reflectance is observed only upon enough crack accumulation. The blue-covered case shown here likely lies just within the removal-and-cracking regimes so that the number of cracks is low enough to not significantly affect reflectance. These observations further extend our earlier inferences on the potential and limitations of using reflectance as an inline process monitoring tool, to colored prints as well. We note that the reflectance or visual appearance of the unprinted paper, for all cases examined here including the black toner, did not change during an observation period of 30 days after unprinting.

The combined effect of fluence and in-plane overlap on the unprinting regime can be quantified using total fluence *E* deposited at an arbitrary location on the paper. The value of *E* can be calculated as per the below relationship.

$$E = \left(\frac{w}{OL}\right)F \quad (2)$$

In this equation, *OL* is the in-plane overlap (in mm), *F* is the pulse fluence (In J/cm²), and *w* is the total width of the optical footprint *w* (≈ 38.1 mm here). Lesser *E* causes partial-removal, too high *E* causes cracking, and an optimum *E* yields the complete-removal regime. Fig. 5d compares *E* corresponding to complete-removal in our experiments, across different print colors. Further, the fluence needed for unprinting black, red-covered and green-covered prints is relatively similar as compared to the much higher value for blue-covered prints. Since the optical absorption of the overprinted samples is very similar to each other and to that of the black print, it is unlikely that the difference in *E* required for complete-removal is an optically governed phenomenon. We further observe that the toner removal process here is more similar in nature to adhesion-

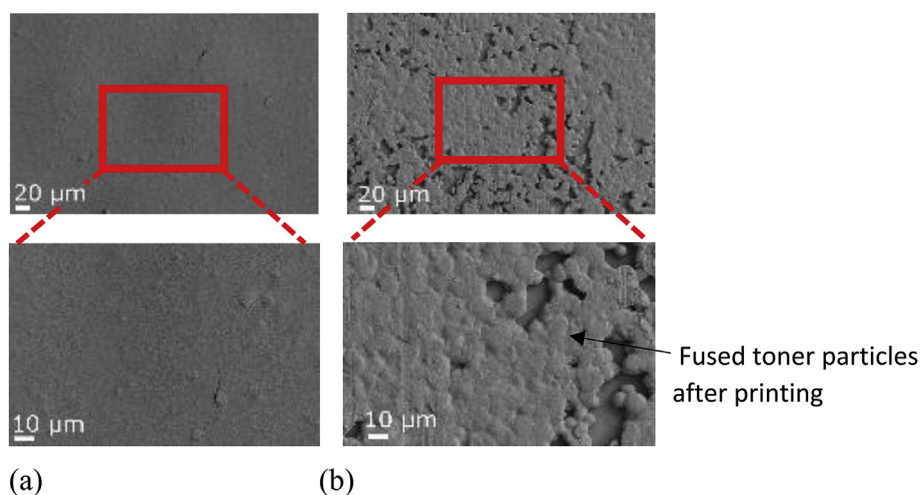


Fig. 6. SEM images of (a) bare paper (b) printed paper with black toner overprinted on red print. (For interpretation of the references to color in this figure legend, the reader is referred to the Web version of this article.)

based unprinting than laser unprinting. In a typical laser printer, the toner particles are deposited in a pattern and then thermally fused to each other and to the coating of the paper. In our unprinting process the pulsed light weakens the paper-toner bond so significantly that a simple ethanol wipe can be used to gently wipe the toner away. This mechanism is evidenced by the fact that the color of the paper did not change until the ethanol wipe was used after pulsed light exposure, and using the wipe before IPL exposure had no effect either. It is therefore likely that a difference in the strength of bonding between the paper and different toner types constituting each color is responsible for the observed trend

in *E* in Fig. 5d.

A typical laser printer uses base toners of Cyan, Magenta and Yellow colors to compose the printed colors examined here, as shown in Table 1. Note that commercial printers commonly use the four-color printing process in which a richer black color is produced using a combination of Cyan, Magenta, Yellow and Black toner (Pring and Campbell, 2000). This is because a combination of 100% Cyan, Magenta and Yellow typically produces only a dark-greyish black color. Since the blue prints do not use yellow toner but the other prints do, the amount of yellow toner in the overprinted samples is relatively lower for the blue-covered case. We

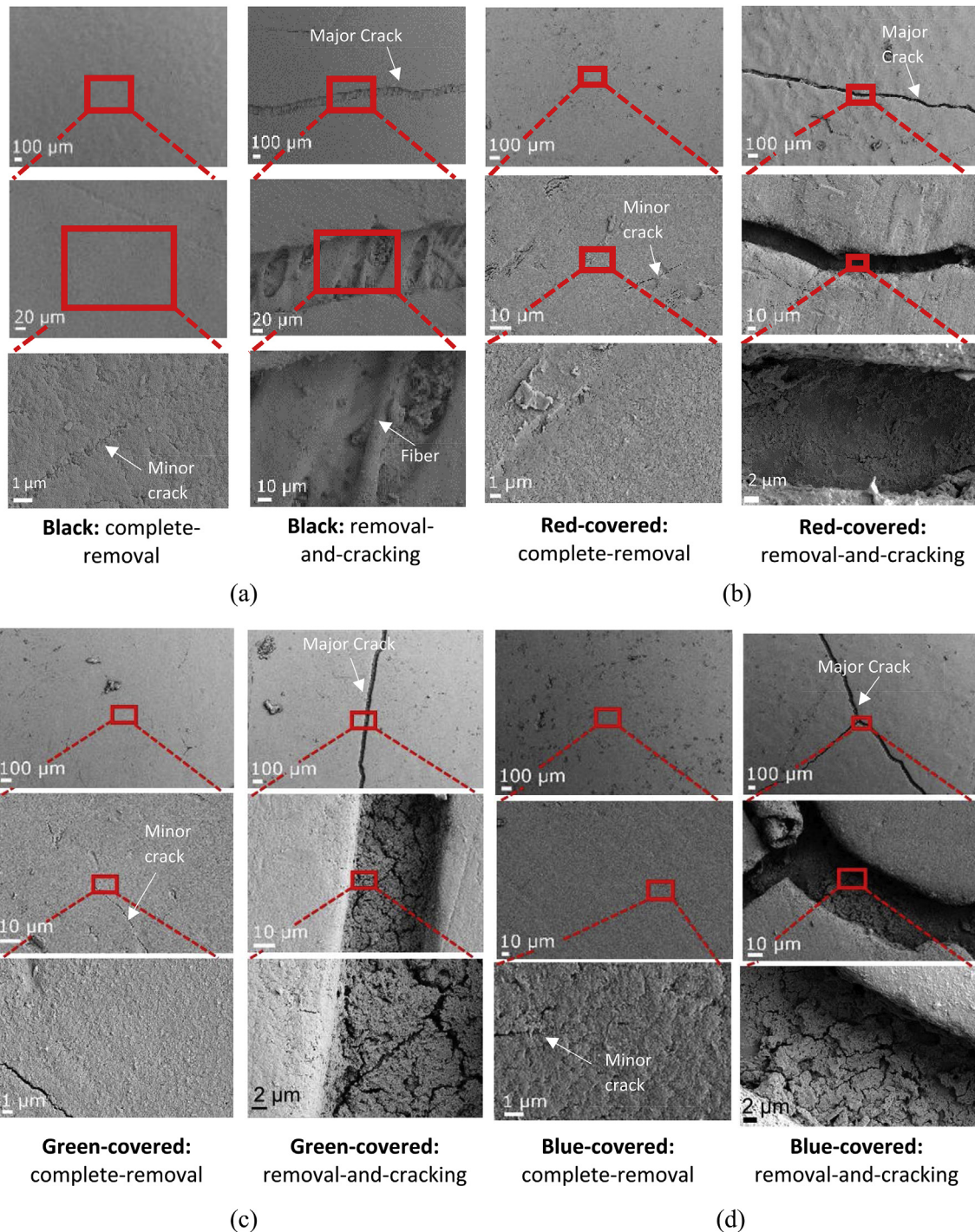


Fig. 7. SEM images of unprinted black and colored-covered cases.

hypothesize that this absence of enough quantity of the yellow toner in the blue prints increases the relative toner-paper bond strength, which results in greater E for complete removal. However, we caution that more evidence of this hypothesis is required by quantitatively examining the toner's chemical composition and its bonding with the paper, which is information that is currently proprietary to the toner manufacturer.

3.2. Paper microstructure

3.2.1. Microscale morphology

SEM images of unprinted paper in the complete-removal and cracking-and-removal regimes were examined to characterize the toner removal and crack evolution on the microscale. Fig. 6a shows SEM images of the bare paper with a smooth surface, which is expected due to the coating which encapsulates the paper fibers. The printed paper (Fig. 6b) shows the fused toner particles on the surface of the coating.

Fig. 7 shows SEM images for complete-removal and removal-and-cracking cases. For complete-removal the toner particles are clearly removed from the coating surface, without the significant morphological damage and removal of the coating that has been observed in laser unprinting (Leal-Ayala et al., 2011). At the same time, minor submicron width cracks appear in the coating. In the

removal-and-cracking regime, the toner is again removed but larger micron-width cracks also appear. The crack morphology shows that the underlying fibers are partially exposed for the black toner, but not for the colored-covered samples. This might be because the overprinting of the additional layer of black toner to the colored prints, before unprinting, limits the depth of damage of the coating. These observations suggest a thermal stress induced mechanism of coating failure in our unprinting process. Smaller cracks emerge in the complete-removal regime due to temperature induced expansion of the coating layer, but are too small in width to significantly affect the appearance and optical properties of the unprinted paper. At larger E and therefore greater temperatures, larger cracks are formed due to greater thermal stresses, thus yielding the removal-and-cracking regime and affecting the optical properties of the paper as well.

We further note that as shown in Fig. 5 the total fluence E for which complete removal is possible is higher than that for removal with a single pulse, e.g., for the case of black prints. This is likely because the use of in-plane overlaps and multiple pulses allows a cooling effect between consecutive pulses that mitigates the thermal-stress induced cracking.

3.2.2. Surface chemistry

ATR-FTIR spectra in Fig. 8 show how the chemical bonds on the

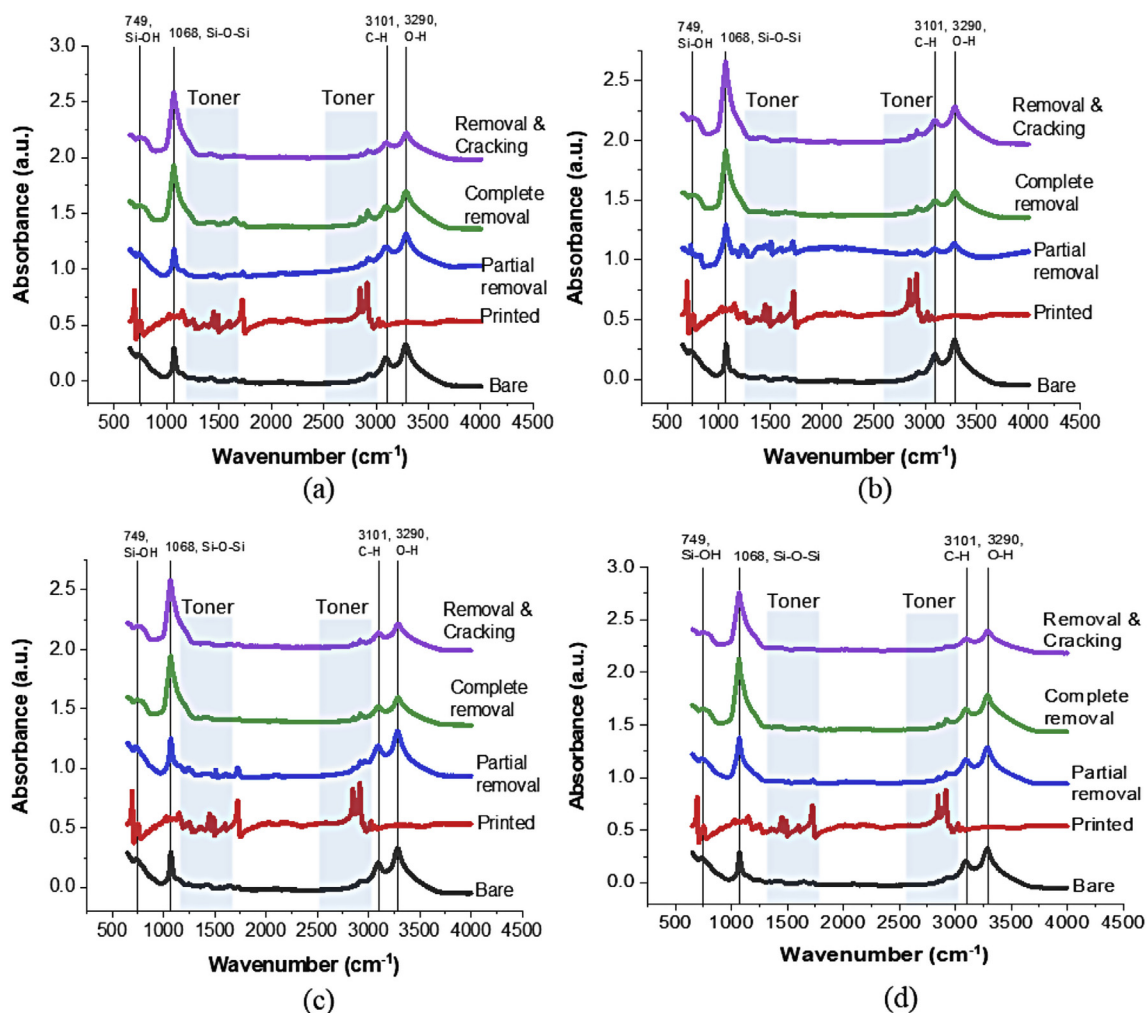


Fig. 8. ATR-FTIR spectra for bare paper, printed samples, and unprinted samples in various unprinting regimes for cases (a) Black (b) Red-covered (c) Green-covered (d) Blue-covered. (For interpretation of the references to color in this figure legend, the reader is referred to the Web version of this article.)

surface of the coated paper change with the unprinting regime. The bare paper shows mainly Si-OH, Si-O-Si, C-H and O-H peaks which are indicated using vertical solid lines. The printed paper has additional peaks corresponding to the constituents of the toner, shown using blue bars. The bare paper peaks are suppressed in the spectra for the printed paper since the penetration depth of ATR-FTIR measurement (typically 0.5–3 μm) is much smaller than typical thickness of deposited toner layers in commercial printing. The spectra in the partial-removal regime shows relatively lower intensity of the toner peaks and reemergence of the coating peaks, indicating exposure of the paper coating. The mitigation of the toner peaks after unprinting is relatively greater for the complete-removal and removal-and-cracking regimes, as expected based on the greater degree of toner removal in these regimes.

The intensity of the Si-OH, Si-O-Si, C-H and O-H peaks is different for the unprinted paper as compared to the bare paper, indicating a change in the chemical bonding after unprinting. To quantify this change, Fig. 9 plots the ratio of intensity I of these peaks in different unprinting regimes to the corresponding peak intensities for the bare paper I_B . From the partial-removal to complete-removal and removal-and-cracking regimes the Si-OH, C-H and O-H peak intensities reduce while the Si-O-Si peak intensity ratio increases significantly. The oxidation of the silica component (increasing Si-O-Si peaks), breakdown of the organic binder (reduction in C-H and O-H peaks) and of the silica-binder bonds (reduction in Si-OH peaks), suggests thermal oxidation induced

breakdown of the coating during unprinting. This causes progressively greater weakening of the paper-toner bond from partial-removal to complete-removal and removal-and-cracking regimes, and lets the toner be easily removed using a simple wipe with low quantity of ethanol in the complete-removal and removal-and-cracking regimes. Note that the use of multiple pulses allows the cumulative fluence to be greater than that in a single pulse, likely because the above thermal cracking is mitigated by the intermediate cooling between consecutive pulses.

Fig. 10 examines the reprintability for paper obtained from ideal IPL unprinting for the different colors examined here. The percentage reduction in photopic reflectance of the unprinted paper with respect to the bare paper indicates how well the toner was removed in a given unprinting cycle. A greater reduction (i.e., more negative value of change) implies a greater change from the white color of the bare paper after IPL unprinting. The percentage change in photopic reflectance after reprinting as compared to the paper printed for the first time indicates the change in appearance of the reprinted paper to the reader. A more positive value of this change over multiple unprinting-reprinting cycles indicates deteriorating readability since the reflectance increases and the absorption of light reduces. Fig. 10 shows that after 5 unprinting-reprinting cycles there is a very significant and large change in reflectance of both the bare paper and of the reprinted paper. This indicates that 5 unprinting cycles is a limit for this paper-toner combination. Therefore, IPL unprinting can reduce the energy usage, chemical

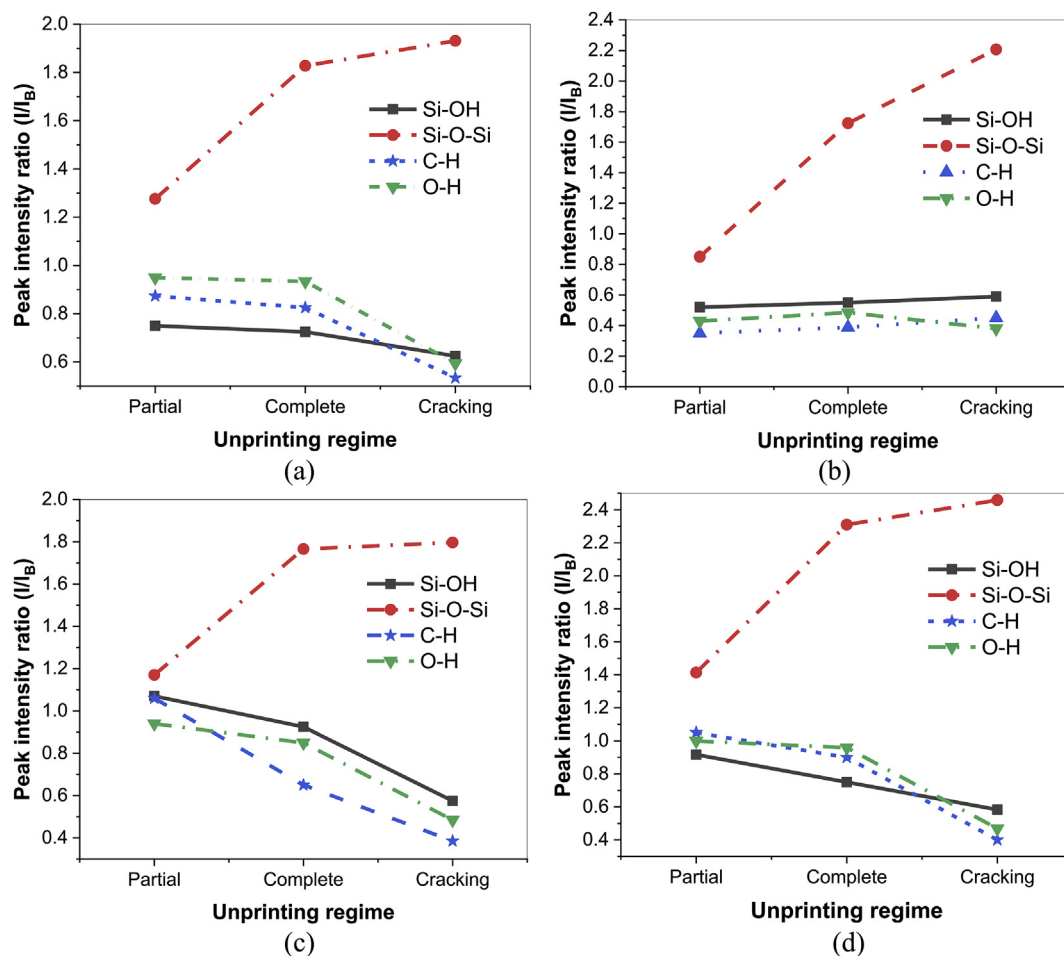


Fig. 9. Ratio of ATR-FTIR peak intensities for different unprinting regimes to corresponding peak intensities for bare paper. (a) Black (b) Red-covered (c) Green-covered (d) Blue-covered. (For interpretation of the references to color in this figure legend, the reader is referred to the Web version of this article.)

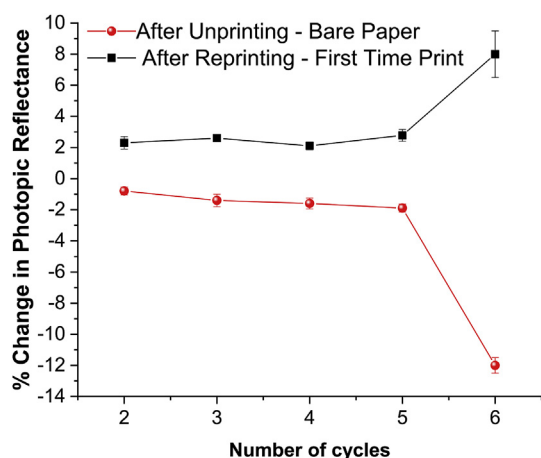


Fig. 10. Comparison of the photopic reflectance from unprinted and reprinted paper to bare paper and first-time printed paper respectively.

pollutant release and climate change emissions involved in conventional recycling of this toner paper combination by about 5 times.

4. Conclusions

This paper demonstrates a new approach for optical unprinting of coated paper with minimal chemical usage (only an ethanol wipe needed). This process can unprint black toner easily, but colored prints are difficult to directly remove due to lower absorption of the IPL by these toners. The overprinting of black toner on colored prints overcomes this issue successfully. Minimal damage or yellowing of the paper and an unprinted reflectance that is very close to that of the bare paper, in the complete-removal regime, show the reusability of the unprinted paper. While this modified approach for unprinting of colors will require additional black toner, the capability of modern printers to overprint patterns accurately and the low process-induced damage on bare paper will reduce the amount of black toner needed. From an in-situ process monitoring point-of-view, increased reflectance can be used as a measure of toner removal and subsequently reduced reflection can indicate occurrence of cracking. However, a key limitation is that cracking only shows a significantly observable reduction in reflectance above a certain amount of crack accumulation.

The following insights into the underlying mechanisms in our unprinting process are also obtained. The FTIR results show an oxidation-based degradation of the coating in the unprinted paper, which progressively increases from partial-removal to complete-removal to occurrence of cracking defects, but also enables the toner to be easily wiped away after IPL exposure. In terms of this mechanism, our unprinting process is closer to adhesion-based unprinting rather than ablation-based laser unprinting. SEM images show initiation of small cracks in the coating even in the complete-removal regime, which grow into much larger cracks that are visible to the human eye upon application of greater fluence in

the removal-and-cracking regime. This suggests that the occurrence and growth of cracks is governed by temperature-induced stresses during the unprinting process. Overall, these observations indicate that the unprinting regime depends on a balance between bond breakage and stress-induced cracking, both of which depend on temperatures and therefore on the cumulative fluence E . Too low E does not allow enough weakening of the toner-paper bonds and results in partial-removal. Higher E enables sufficient weakening of the bonds to allow wiping away of toner, yielding the complete-removal regime, but also causes minor cracks to initiate due to the higher temperatures involved. Even higher total fluence supplies sufficient energy for bond breakage but also activates greater degree of temperature-induced cracking, resulting in the removal-and-cracking regime. Along the same lines, the dependence of E for complete-removal on the color in colored-overprinted samples is likely due to a change in the bonding strength between the paper coating and the combination of toners used to create the color.

The process throughput in the complete-removal regime, based on the experiments performed here, is shown in Table 2. The throughput was calculated based on the area of the bar printed. Since the largest dimension of the optical footprint of IPL is much bigger (12 inches here) the potential process throughput is much higher. Nevertheless, this calculation does allow us to compare the process speed to that of the successful laser unprinting process. Past work (Leal-Ayala et al., 2011) used a 532 nm laser with a spot area of $2.25 \times 10^{-4} \text{ cm}^2$, laser scan speed of $150 \mu\text{m/s}$ and line spacing of $50 \mu\text{m}$ for successfully unprinting uncoated paper. The highest throughput obtained was $7500 \mu\text{m}^2/\text{s}$. In comparison, the throughput achieved in our process is orders of magnitude higher, as is evident from Table 2. Overall, IPL unprinting has all the advantages of laser unprinting, and the additional ability to achieve damage-free unprinting of coated paper with significantly higher throughput. Given the availability of xenon lamps in various sizes similar to scanners in commercial printer systems, IPL unprinting is also amenable to integration with conventional printers for realizing unprinting in an automated manner within a point-of-use setting.

However, we caution against assuming that our process can completely replace laser unprinting or conventional recycling. Our process was unable to unprint toner of any color from non-coated paper, unlike laser unprinting. Nonetheless, given the high consumption of coated printing paper the developed IPL unprinting process is ideally suited to act as a scalable complement to laser unprinting and may enhance the potential sustainability achieved by it even further. Secondly, IPL unprinting cannot be done an infinite number of times, as shown in Fig. 10. For the toner-paper combination used here we find that unprinting-reprinting is possible at least 5 times without significant damage to the paper. This limit is very close to the number of times paper can be recycled (5–6 times as per the U.S. Environmental Protection Agency) using the conventional recycling approach. This indicates that our unprinting approach could enable about 5 times reduction in the energy usage, pollutant release and climate change emission as compared to conventional recycling with relatively little change in the number of times that reuse is possible. This represents a very

Table 2
Pulsed light parameters and throughput for complete-removal regimes.

Unprinting Case	On-time (μs)	Off-time (s)	No. of overlap	Throughput (mm^2/s)
Black	1700	1.15	4	2.8
Red-Covered	2440	2.44	3	1.75
Green-Covered	1250	0.83	5	3.08
Blue-Covered	1450	0.96	8	1.67

significant reduction but not complete elimination of the conventional recycling process. Further, fully quantifying the potential of IPL unprinting and robustly confirming the unprinting mechanisms requires testing of a wider variety of paper-toner combinations, which is a subject of future work.

Acknowledgements

This work was supported by the National Science Foundation, USA, grants CMMI #1809289 and CBET #1449383. High school students Shweta Nair from Cherokee High School and Ethan Sirak from South Hunterdon Regional High School also performed some preliminary unprinting experiments. We are grateful for the support by the SLAAM program in the Rutgers Department of Mechanical and Aerospace Engineering for the support provided for their participation.

Appendix A. Supplementary data

Supplementary data to this article can be found online at <https://doi.org/10.1016/j.jclepro.2019.05.387>.

References

- Ahmadi, A., Williamson, B.H., Theis, T.L., Powers, S.E., 2003. Life-cycle inventory of toner produced for xerographic processes. *J. Clean. Prod.* 11 (5), 573–582.
- Bajpai, P., 2014. 7 - chemicals used in deinking and their Function**Some excerpts taken from Bajpai, 2006 with kind permission from Pira International, UK. In: Bajpai, P. (Ed.), *Recycling and Deinking of Recovered Paper*. Elsevier, Oxford, pp. 121–137.
- Bansal, S., Malhotra, R., 2016. Nanoscale-shape-mediated coupling between temperature and densification in intense pulsed light sintering. *Nanotechnology* 27 (49), 495602.
- Bhatia, S., Pichel, M., Ashu, J.T., 1999. Method and Apparatus for Deinking Paper, Worldwide Patent WO9947743. Assigned to De-copier Technologies Inc. (US).
- Boyce, J.B., Noolandi, J., Mei, P., 2001. Method and Apparatus of Recycling Office Paper, U.S. Patent US6236831. Assigned to Xerox Corporation.
- Counsell, T.A.M., Allwood, J.M., 2006. Desktop paper recycling: a survey of novel technologies that might recycle office paper within the office. *J. Mater. Process. Technol.* 173 (1), 111–123.
- Counsell, T.A.M., Allwood, J.M., 2007. Reducing climate change gas emissions by cutting out stages in the life cycle of office paper. *Resour. Conserv. Recycl.* 49 (4), 340–352.
- Counsell, T.A.M., Allwood, J.M., 2008. Meeting the 2050 carbon target for paper by print removal. *CIRP Annals* 57 (1), 25–28.
- Dexter, M., Gao, Z., Bansal, S., Chang, C.-H., Malhotra, R., 2018. Temperature, crystalline phase and influence of substrate properties in intense pulsed light sintering of copper sulfide nanoparticle thin films. *Sci. Rep.* 8 (1), 2201.
- Dharmadasa, R., Jha, M., Amos, D.A., Druffel, T., 2013. Room temperature synthesis of a copper ink for the intense pulsed light sintering of conductive copper films. *ACS Appl. Mater. Interfaces* 5 (24), 13227–13234.
- EIPPCB, 2001. Reference Document on Best Available Techniques in the Pulp and Paper Industry. European Integrated Pollution Prevention and Control Bureau.
- Energetics Incorporated Columbia, M., 2005. ITP Forest Products: Energy and Environmental Profile of the U.S. Pulp and Paper Industry, Fujiwara, T., Yamaoka, C., Yoshie, N., 2000. Recyclable Image-Recording Medium. European Patent EP1020772. Assigned to Minolta Co. Ltd. (Japan).
- Greenberg, B.L., Robinson, Z.L., Reich, K.V., Gorynski, C., Voigt, B.N., Francis, L.F., Shklovskii, B.I., Aydil, E.S., Kortshagen, U.R., 2017. ZnO nanocrystal networks near the insulator–metal transition: tuning contact radius and Electron density with intense pulsed light. *Nano Lett.* 17 (8), 4634–4642.
- Hirai, A., 2002. Apparatus and Method for Removing a Print Material on a Recording Medium, European Patent EP1168106. Assigned to Minolta Co. Ltd. (Japan).
- Jha, M., Dharmadasa, R., Draper, G.L., Sherehiy, A., Sumanasekera, G., Amos, D., Druffel, T., 2015. Solution phase synthesis and intense pulsed light sintering and reduction of a copper oxide ink with an encapsulating nickel oxide barrier. *Nanotechnology* 26 (17), 17560101–17560110.
- Jiang, C., Ma, J., 2000. DE-INKING OF WASTE PAPER: FLOTATION. In: Wilson, I.D. (Ed.), *Encyclopedia of Separation Science*. Academic Press, Oxford, pp. 2537–2544.
- Kang, H., Sowade, E., Baumann, R.R., 2014. Direct intense pulsed light sintering of inkjet-printed copper oxide layers within six milliseconds. *ACS Appl. Mater. Interfaces* 6 (3), 1682–1687.
- Leal-Ayala, D.R., Allwood, J.M., Counsell, T.A.M., 2011. Paper un-printing: using lasers to remove toner-print in order to reuse office paper. *Appl. Phys. A* 105 (4), 801–818.
- Leal-Ayala, D.R., Allwood, J.M., Schmidt, M., Alexeev, I., 2012. Toner-print removal from paper by long and ultrashort pulsed lasers. In: *Proceedings of the Royal Society A*, pp. 2272–2293.
- Lehtinen, E., 2000. Kaolin. In: Gullichsen, J., Paulapuro, H. (Eds.), *Pigment Coating and Surface Sizing of Paper*. Fapet Oy.
- MacNeill, W., Choi, C.-H., Chang, C.-H., Malhotra, R., 2015. On the self-damping nature of densification in photonic sintering of nanoparticles. *Sci. Rep.* 5, 1484501–1484513.
- Man, Y., Shen, W., Chen, X., Long, Z., Pons, M.-N., 2017. Modeling and simulation of the industrial sequencing batch reactor wastewater treatment process for cleaner production in pulp and paper mills. *J. Clean. Prod.* 167, 643–652.
- Metz, B., Davidson, O.R., Bosch, P.R., Dave, R., Meyer, L.A., 2007. *Climate Change 2007: Mitigation of Climate Change*. Contribution of Working Group III to the Fourth Assessment Report of the Intergovernmental Panel on Climate Change. Cambridge University Press.
- Mitsubishi, K., Yamada, D., Ohnishi, M.M.D., 1994. Rewritable Recording Device, European Patent EP0583483. Assigned to Mitsubishi Electric Corp. (Japan).
- Nair, M.T.S., Nair, P.K., 1989. Chemical bath deposition of CuS thin films and their prospective large area applications. *Semicond. Sci. Technol.* 4, 191–199.
- Nathan, V.K., Rani, M.E., Gunaseeli, R., Kannan, N.D., 2018. Enhanced biobleaching efficacy and heavy metal remediation through enzyme mediated lab-scale paper pulp deinking process. *J. Clean. Prod.* 203, 926–932.
- Nations, U., 2016. *Pulp and Paper Capacities*, pp. 1–184.
- Pring, R., Campbell, A., 2000. *Watson-Guption*. www.color.com.
- Singh, S.K., Kulkarni, S., Kumar, V., Vashistha, P., 2018. Sustainable utilization of deinking paper mill sludge for the manufacture of building bricks. *J. Clean. Prod.* 204, 321–333.
- Tesfaye, T., Sithole, B., Ramjugernath, D., Chunilall, V., 2017. Valorisation of chicken feathers: application in paper production. *J. Clean. Prod.* 164, 1324–1331.
- Tong, X., Shen, W., Chen, X., Corriou, J.-P., 2018. Qualitative and quantitative analysis of gaseous pollutants for cleaner production in pulp and paper mills. *J. Clean. Prod.* 198, 1066–1075.
- Tsatsis, D.E., Papachristos, D.K., Valta, K.A., Vlyssides, A.G., Economides, D.G., 2017. Enzymatic deinking for recycling of office waste paper. *J. Environ. Chem. Eng.* 5 (2), 1744–1753.
- Wan-Ho, C., Hyun-Jun, H., Seung-Hyun, L., Hak-Sung, K., 2013. In situ monitoring of a flash light sintering process using silver nano-ink for producing flexible electronics. *Nanotechnology* 24 (3), 03520201–03520208.
- Yoshie, N., Taniguchi, K., 2000. Apparatus for Removing Printing Material from a Recording Member on Which an Image Is Recorded by the Printing Material, United States Patent Office US6128464. Minolta Co. Ltd. (Japan).